NN correlations and relativistic Hartree-Fock in finite nuclei

R. Fritz and H. Müther
Institut für Theoretische Physik, Universität Tübingen, D-72076 Tübingen, Germany
(Received 28 September 1993)

Two different approximation schemes for the self-consistent solution of the relativistic Brueckner-Hartree-Fock equation for finite nuclei are discussed using realistic one-boson-exchange potentials. In a first scheme, the effects of correlations are deduced from a study of nuclear matter and parametrized in terms of an effective σ, ω, and π exchange. Employing this effective interaction relativistic Hartree-Fock equations are solved for finite nuclei ^{16}O, ^{40}Ca, and ^{48}Ca. In the second approach the effect of correlations are treated in the Brueckner-Hartree-Fock approximation directly for the finite nuclei, but the modifications of the Dirac spinors in the medium are derived from nuclear matter assuming a local-density approximation. Both approaches yield rather similar results for binding energies and radii in fair agreement with experimental data. The importance of the density dependent correlation effects is demonstrated and different ingredients to the spin-orbit splitting in the shell model of the nucleus are discussed.

PACS number(s): 21.60.Jz, 21.10.Dr, 21.10.Ft, 21.65.+f

I. INTRODUCTION

The various attempts to derive the bulk properties of nuclear systems from realistic nucleon-nucleon (NN) interactions are confronted with two major obstacles. The first one is the necessity to consider the effects of NN correlations which are due to the strong short-range and tensor components in a realistic NN interaction. The second one is of a relativistic nature: The strong scalar-meson (σ) exchange part required in realistic meson-exchange potentials [1,2] gives rise to a significant modification of the Dirac structure of nucleons in the nuclear medium [3]. Therefore relativistic features should be included in the many-body theory of nuclear systems, in order to account for this effect.

The importance of the NN correlations is made obvious by the fact that no binding energy of nuclear systems is obtained if these correlations are ignored: A Hartree-Fock (HF) calculation employing, e.g., a realistic one-boson-exchange (OBE) potential [2], which fits NN scattering data, yields unbound nuclei. Various methods have been developed to include the effects of two-nucleon correlations. One possibility is the so-called Brueckner-Hartree-Fock (BHF) approximation. In this approach one considers a Slater determinant, which should be an appropriate model wave function for the nuclear system to be investigated. Solving the Bethe-Goldstone equation yields an effective interaction, the G matrix, which depends on the bare NN interaction and the model wave function considered. The self-consistency condition of BHF now requires that the model wave function, which is needed to set up the Bethe-Goldstone equation, be made identical to the solution of the HF equations using the G matrix as a kind of effective interaction.

This self-consistency problem is simplified for nuclear matter since the translational symmetry of this infinite system requires plane waves for the single-particle wave functions to build up the Slater determinant. For many years, however, the BHF self-consistency problem has also been solved for finite nuclei [4,5].

The inclusion of NN correlations led to a substantial improvement in the microscopic description of bulk properties of nuclei. For both nuclear matter as well as finite nuclei BHF calculations employing various realistic NN interactions gave results which were located on the so-called Coester band [6,7]. This means that either the calculated binding energy turned out to be too small or the calculated radii were too small (which corresponds to a saturation density of nuclear matter too large) as compared to the experimental data. Attempts have been made to improve the many-body approach such that results "off the Coester band," closer to the experimental data, were obtained. Such attempts have been made within the hole-line expansion of the Brueckner theory [8] or using different schemes [9–11]. Even today it is not really clear if it is possible to derive the bulk properties of nuclear systems from realistic NN forces within a nonrelativistic many-body theory [12].

Motivated by the success of the phenomenological σ-ω model of Serot and Walecka [3], attempts have been made to incorporate the relativistic features of this approach also in nuclear structure calculations which are based upon realistic NN forces. In this approach, one accounts for the fact that the relativistic nucleon self-energy in a nuclear medium is given essentially by a large attractive component, originating mainly from the exchange of the scalar σ meson and therefore transforming like a scalar under a Lorentz transformation, and a repulsive component, which transforms like the zero component of a Lorentz vector and is mainly due to the exchange of the ω meson. The single-particle motion is described by a Dirac equation which includes this self-energy. The strong components of the self-energy yield solutions of the Dirac equation, which are quite different from the Dirac spinors describing the nucleons in the vacuum.

This change of the Dirac spinors in the medium gives

rise to a self-consistency problem beyond the one already discussed above: Already in evaluating the matrix elements of the bare NN force V one should know the structure of the Dirac spinors, resulting from the solution of the Dirac equation. Again, this self-consistency problem is highly simplified in nuclear matter. In this case the medium dependence of the Dirac spinors is characterized by an effective mass, which represents the ratio of the small to the large component of the spinor.

Such Dirac BHF (DBHF) calculations have been performed for nuclear matter by, e.g., Shakin and collaborators [13], Brockmann and Machleidt [14], and ter Haar and Malfliet [15]. The basic aspects of this approach have been thoroughly investigated by Horowitz and Serot [16]. Due to the scalar field, the nucleon mass is reduced, enhancing the ratio between small and large components of the Dirac spinors. This change in the Dirac spinors yields a reduction of the scalar density, which implies that the attraction due to the exchange of the σ meson in OBE potentials is reduced. At small densities of nuclear matter this loss of attraction is counterbalanced by a reduction of the kinetic energy, which is also caused by the medium dependence of the Dirac spinors. At larger densities the loss of attraction in the NN interaction overwhelms the loss of repulsion in the kinetic energy and for those densities the energy calculated in the DBHF approximation is less attractive than the corresponding energy calculated in the BHF approximation, ignoring these relativistic effects.

Consequently, the saturation points calculated for nuclear matter in the DBHF approximation are shifted to smaller densities as compared to the BHF result. Brockmann and Machleidt succeeded in constructing a realistic OBE potential which fits NN scattering data and also yields DBHF results for nuclear matter in satisfying agreement with the empirical data [14]. The same feature is also observed for the potential A, defined in Table A.2 of Ref. [2], which we will consider also in our present investigation.

This success of the DBHF approximation in nuclear matter gives rise in the hope that the same DBHF approximation may also be successful in reproducing the binding energies and radii of finite nuclei. From the discussion above, it is obvious, however, that a complete self-consistent calculation for finite nuclei is rather involved. Therefore we are going to investigate two approximations, in which either the effects of correlations or the relativistic effects are taken from studies of nuclear matter, while the respective other components of the calculation are treated in a self-consistent way directly for the finite nuclei.

In the first approximation, we determine an effective meson theory (σ, ω, and π mesons), which yields in a Hartree-Fock approximation for nuclear matter at a given density ρ the same observables for the self-energy of the nucleons and the binding energy as a DBHF calculation of nuclear matter. This leads to a set of coupling constants, which depend on the nuclear density. This density dependence reflects the density dependence of the correlations described by the G matrix of DBHF. Keeping track of the density dependence of these coupling constants one can perform a relativistic HF calculation using techniques as described, e.g., by Bouyssy *et al.* [17]. A calculation along this line has been performed by Brockmann and Toki [18] restricted to a Hartree description and first results of a HF calculation have been presented in [19]. Both of these earlier investigations allowed for an exchange of effective σ and ω mesons, only.

In the second approximation one is expanding the single-particle wave functions of a self-consistent BHF calculation for finite nuclei in a basis of plane waves. The Dirac structure of these plane waves is taken from the corresponding state in nuclear matter of a density, which is equal to the average density for the single-particle orbit in the finite nucleus under consideration. In this way one deduces the Dirac effects from nuclear matter, but otherwise performs a complete self-consistent BHF calculation. This approach has also been used in Ref. [20].

It turns out that these two very different approximations yield rather similar results. Therefore one can assume that a result of complete DBHF calculation should also be close. It is the main aim of the present investigation to explore the differences between the two approaches in a systematic way. For that purpose we are studying results on various nuclei (^{16}O, ^{40}Ca, ^{48}Ca) using different OBE interactions (OBE potentials A and C defined in Table A.2 of [2]). After this Introduction we define the details of the two approximations towards a self-consistent DBHF calculation for finite nuclei in Secs. II and III, respectively. The results are presented and discussed in Sec. IV and the main conclusions are summarized in Sec. V.

II. EFFECTIVE MESON-EXCHANGE APPROACH

Our starting point for the description of the nuclear many-body problem is the effective Lagrangian density for the interacting nucleons and the σ, ω, and π mesons,

$$\mathcal{L} = \mathcal{L}_0 + \mathcal{L}_{\rm I} \,, \tag{1}$$

consisting of the free Lagrangian density

$$\begin{aligned}\mathcal{L}_0 = {} & \overline{\Psi}(i\gamma_\mu\partial^\mu - M)\Psi + \frac{1}{2}(\partial_\mu\Phi_\sigma\partial^\mu\Phi_\sigma - m_\sigma^2\Phi_\sigma^2) \\ & + \frac{1}{2}m_\omega^2\Phi_{\omega,\mu}\Phi_\omega^\mu - \frac{1}{4}F_{\mu\nu}F^{\mu\nu} \\ & + \frac{1}{2}(\partial_\mu\Phi_\pi\partial^\mu\Phi_\pi - m_\pi^2\Phi_\pi^2) \,,\end{aligned} \tag{2}$$

with

$$F_{\mu\nu} = \partial_\mu\Phi_{\omega,\nu} - \partial_\nu\Phi_{\omega,\mu} \,, \tag{3}$$

and the interaction Lagrangian density

$$\mathcal{L}_{\rm I} = -G_\sigma\overline{\Psi}\Phi_\sigma\Psi - G_\omega\overline{\Psi}\gamma_\mu\Phi_\omega^\mu\Psi - \frac{f_\pi}{m_\pi}\overline{\Psi}\gamma_5\gamma_\mu(\partial^\mu\Phi_\pi)\Psi \,. \tag{4}$$

The nucleon field and rest mass are denoted by Ψ and M, whereas the meson fields, rest masses, and effective nucleon-meson coupling constants are denoted by Φ_i, m_i,

and G_i or f_i with $i = \{\sigma, \omega, \pi\}$ for the scalar, vector, and pseudoscalar mesons, respectively. Note that for the pion we use the pseudovector coupling and suppress the notations for the isospin degrees of freedom. Moreover, we already mention here that we will subtract the zero-range part in the one-pion-exchange contributions to the NN interaction. This is done to account for the effects of short-range correlations between the interacting nucleons.

A. Nuclear matter

Following standard techniques [3,17], the Hartree-Fock approximation for this Lagrangian leads to a Dirac equation for nucleons with four-momentum $p = (p^0, \mathbf{p})$ in nuclear matter,

$$[\boldsymbol{\gamma} \cdot \mathbf{p} + M + \Sigma(p)]\Psi(\mathbf{p}, s) = \gamma_0 E(\mathbf{p})\Psi(\mathbf{p}, s) \ , \tag{5}$$

for the nucleon spinors $\Psi(\mathbf{p}, s)$, containing the self-energy $\Sigma(p)$. Because of the isotropy of nuclear matter, the spinors $\Psi(\mathbf{p}, s)$ are known to be plane waves and in the rest frame of nuclear matter, the self-energy $\Sigma(p)$ for on-shell nucleons $[p^0 = E(\mathbf{p})]$ depends only on the absolute value of the three-momentum $\mathbf{p}$. This nucleon self-energy can be split into different parts with a well-defined behavior under Lorentz transformations. Because of parity conservation, time reversal invariance, and Hermiticity, the most general form of $\Sigma(\mathbf{p})$ is restricted to

$$\Sigma(\mathbf{p}) = \Sigma^s(\mathbf{p}) - \gamma^0\Sigma^0(\mathbf{p}) + \boldsymbol{\gamma}\cdot\mathbf{p}\Sigma^v(\mathbf{p}) \ , \tag{6}$$

with $\Sigma^s(p)$, $\Sigma^0(p)$, and $\Sigma^v(p)$ transforming like Lorentz scalars. Therefore the Dirac equation can be rewritten as

$$[\boldsymbol{\gamma}\cdot\mathbf{p}^* + M^*(\mathbf{p})]\Psi(\mathbf{p}, s) = \gamma_0 E(\mathbf{p})^*\Psi(\mathbf{p}, s) \ , \tag{7}$$

introducing the definitions

$$\begin{aligned} \mathbf{p}^* &= \mathbf{p}\,[1 + \Sigma^v(\mathbf{p})] \ , \\ M^*(\mathbf{p}) &= M + \Sigma^s(\mathbf{p}) \ , \\ E^*(\mathbf{p}) &= E(\mathbf{p}) + \Sigma^0(\mathbf{p}) \ . \end{aligned} \tag{8}$$

The formal similarity with a free Dirac equation allows one immediately to determine the nucleon spinor in nuclear matter to

$$\Psi(\mathbf{p}, s) = \left(\frac{E^*(\mathbf{p}) + M^*(\mathbf{p})}{2E^*(\mathbf{p})}\right)^{1/2} \begin{pmatrix} 1 \\ \frac{\boldsymbol{\sigma}\cdot\mathbf{p}^*}{E^*(\mathbf{p})+M^*(\mathbf{p})} \end{pmatrix} \chi^s \ , \tag{9}$$

now with a modified ratio of the spinor upper and lower components if compared with the vacuum solution. The spinors are normalized (noncovariant) to

$$\Psi(\mathbf{p}, s)^\dagger\Psi(\mathbf{p}, s) = 1 \ , \quad \overline{\Psi}(\mathbf{p}, s)\Psi(\mathbf{p}, s) = \frac{M^*(\mathbf{p})}{E^*(\mathbf{p})} \ , \tag{10}$$

and the on-shell condition in nuclear matter now reads like

$$E^*(\mathbf{p})^2 = M^*(\mathbf{p})^2 + \mathbf{p}^{*2} \ . \tag{11}$$

On the level of the Hartree-Fock approximation, the mesons used in our Lagrange density give rise to the following contributions to the self-energy:

$$\Sigma^s(\mathbf{p}) = -\left(\frac{G_\sigma}{m_\sigma}\right)^2 \rho_s + \frac{1}{(4\pi)^2}\frac{1}{p}\int_0^{k_F} q dq \frac{M^*(q)}{E^*(q)}\left[G_\sigma^2\Theta_\sigma(p,q) - 4G_\omega^2\Theta_\omega(p,q) - 3\left(\frac{f_\pi}{m_\pi}\right)^2 m_\pi^2\Theta_\pi(p,q)\right] \ , \tag{12}$$

$$\Sigma^0(\mathbf{p}) = -\left(\frac{G_\omega}{m_\omega}\right)^2 \rho - \frac{1}{(4\pi)^2}\frac{1}{p}\int_0^{k_F} q dq\left[G_\sigma^2\Theta_\sigma(p,q) + 2G_\omega^2\Theta_\omega(p,q) - 3\left(\frac{f_\pi}{m_\pi}\right)^2 m_\pi^2\Theta_\pi(p,q)\right], \tag{13}$$

$$\Sigma^v(\mathbf{p}) = -\frac{1}{(4\pi p)^2}\int_0^{k_F} q dq \frac{q^*}{E^*(q)}\left[2G_\sigma^2\Gamma_\sigma(p,q) + 4G_\omega^2\Gamma_\omega(p,q) - 6\left(\frac{f_\pi}{m_\pi}\right)^2\left[(p^2+q^2)\Gamma_\pi(p,q) - pq\Theta_\pi(p,q)\right]\right] . \tag{14}$$

We omit in our notation the obvious dependence of the self-energies on the Fermi momentum k_F. The first term in $\Sigma^s(\mathbf{p})$ and $\Sigma^0(\mathbf{p})$ corresponds to the Hartree contribution using

$$\rho(k_F) = \frac{2}{3\pi^2}k_F^3 \quad \text{and} \quad \rho_s(k_F) = \frac{2}{\pi^2}\int_0^{k_F} q^2 dq \frac{M^*(q)}{E^*(q)} \tag{15}$$

for the baryon and scalar density, respectively. The remaining expressions are due to the Fock (exchange) contributions where we have used the abbreviations

$$A_i(p,q) = p^2 + q^2 + m_i^2 - [E(p) - E(q)]^2 \ , \tag{16}$$

$$\Theta_i(p,q) = \ln\left(\frac{A_i(p,q) + 2pq}{A_i(p,q) - 2pq}\right) \ , \tag{17}$$

$$\Gamma_i(p,q) = \frac{A_i(p,q)\Theta_i(p,q)}{4pq} - 1 \ ; \tag{18}$$

again $i = \{\sigma, \omega, \pi\}$. Two important things have to be noted. First, as already mentioned above, we have subtracted zero-range contributions from pion exchange to the self-energy $\Sigma(\mathbf{p})$. Second, we do not want to consider retardation effects in the meson propagators. Although retardation causes no problems in nuclear matter, the neglect leads to significant simplifications in finite nuclei.

In the next step we determine effective coupling constants G_σ and G_ω for the scalar and vector mesons by requesting that the HF expressions for the scalar self-energy $\Sigma^s(\mathbf{p})$ calculated at the Fermi surface ($p = k_f$) and the binding energy per nucleon reproduce the corresponding results of a Dirac-Brueckner-HF (DBHF) calcu-

lation [2,14] using realistic NN forces, namely, versions A and C of the Bonn potential [2]. For the pion we fix the coupling constant to the free value $f_\pi^2/4\pi = 0.08$ and the masses of the mesons are chosen to be identical to those of the OBE potential (m_π=138 MeV, m_σ=550 MeV, and m_ω=783 MeV). In this way we obtain for each baryon density ρ two effective coupling constants $G_\sigma(\rho)$ and $G_\omega(\rho)$. The density dependence of these coupling constants reflects the density dependence of the correlations taken into account in the DBHF approximation.

B. Finite nuclei

Once the density-dependent coupling constants are determined, we assume for the study of finite nuclei that we can account for the density-dependent correlation effects in a relativistic HF calculation by employing the coupling constants calculated at the local density $G_\sigma(\rho(r))$ and $G_\omega(\rho(r))$, where the density profile $\rho(r)$ is determined from the result of the relativistic HF calculation in a self-consistent manner. For that purpose we write the nucleon spinor for the finite system in coordinate space,

$$\langle r|\alpha\rangle = \Psi_\alpha(\mathbf{r}) = \begin{pmatrix} g_a(r) \\ -if_a(r)\,\sigma\cdot\hat{\mathbf{r}} \end{pmatrix} \mathcal{Y}_{\kappa_a,m_a}(\Omega)\,\chi_{\frac{1}{2},(q_a)} \tag{19}$$

$$= \begin{pmatrix} g_a(r)\,\mathcal{Y}_{\kappa_a,m_a}(\Omega) \\ if_a(r)\,\mathcal{Y}_{-\kappa_a,m_a}(\Omega) \end{pmatrix} \chi_{\frac{1}{2},(q_a)} \,. \tag{20}$$

Again, the spinors are normalized to

$$\int d^3\mathbf{r}\Psi^\dagger(\mathbf{r})\Psi(\mathbf{r}) = \int_0^\infty r^2dr\,[g_a^2(r) + f_a^2(r)] = 1 \,. \tag{21}$$

All quantum numbers are summarized by the index $\alpha = \{a, m_a\}$ with $a = \{n_a, \kappa_a, q_a\}$. n_a characterizes the radial quantum numbers, whereas $\kappa_a = (2j_a+1)(l_a - j_a)$ describes the angular momenta. Obviously the upper and lower spinor components for the same total angular momentum j_a have different orbital quantum numbers l_a. We introduce the corresponding l'_a to the same j_a,

$$l'_a = \begin{cases} l_a + 1 \text{ for } l_a = j_a - \frac{1}{2} \,, \\ l_a - 1 \text{ for } l_a = j_a + \frac{1}{2} \,, \end{cases} \tag{22}$$

and $a' = \{n_a, \kappa'_a, q_a\}$, $\kappa'_a = (2j_a+1)(l'_a - j_a)$. $\mathcal{Y}_{\kappa_a,m_a}(\Omega)$ is constructed as usual,

$$\mathcal{Y}_{\kappa_a,m_a}(\Omega) = \sum_{m_l,m_s} (l_a m_l\ \tfrac{1}{2}\ m_s|j_a m_a) Y_{l_a,m_l}(\Omega)\chi_{\frac{1}{2},m_s} \,. \tag{23}$$

For the isospinor $\chi_{\frac{1}{2},(q_a)}$ we use

$$q_a = \begin{cases} +1 \text{ for protons} \,, \\ -1 \text{ for neutrons} \,. \end{cases} \tag{24}$$

The Dirac equation is solved by expanding the radial functions $g_a(r)$ and $f_a(r)$ in a discrete basis of spherical Bessel functions. The wave numbers for this basis are chosen such that this discrete basis is a complete orthonormal basis in a sphere of radius D. This radius is chosen to be large enough that the results for the bound single-particle states are independent on D. With this expansion the Dirac equation (5) is rewritten in form of an eigenvalue problem and the eigenvalues (E_a) and eigenvectors (the expansion coefficients for g_a and f_a) are determined by a simple matrix diagonalization [21].

In the following we give the expressions for the matrix elements of the self-energy in this Dirac matrix, calculated in the Hartree-Fock approximation. In this work we consider nuclei with a closed proton and neutron shell only. Therefore, the isovector pseudoscalar meson yields no contributions in the Hartree approximation. The Hartree matrix elements for the isoscalar scalar and vector parts of the interaction and the Coulomb force are given as

$$\langle\alpha|\Sigma_\sigma^H|\beta\rangle = -\delta_{\kappa_a,\kappa_b}\delta_{m_a,m_b}\delta_{q_a,q_b}\int_0^\infty r^2drG_\sigma(r)\,[g_a(r)g_b(r) - f_a(r)f_b(r)]$$
$$\times\left\{m_\sigma\int_0^\infty r'^2dr'G_\sigma(r')\rho_s(r')\widetilde{I}_0(m_\sigma r_<)\widetilde{K}_0(m_\sigma r_>)\right\} \,, \tag{25}$$

$$\langle\alpha|\Sigma_\omega^H|\beta\rangle = \delta_{\kappa_a,\kappa_b}\delta_{m_a,m_b}\delta_{q_a,q_b}\int_0^\infty r^2drG_\omega(r)\,[g_a(r)g_b(r) + f_a(r)f_b(r)]$$
$$\times\left\{m_\omega\int_0^\infty r'^2dr'G_\omega(r')\rho(r')\widetilde{I}_0(m_\omega r_<)\widetilde{K}_0(m_\omega r_>)\right\} \,, \tag{26}$$

$$\langle\alpha|\Sigma_c^H|\beta\rangle = \delta_{\kappa_a,\kappa_b}\delta_{m_a,m_b}\int_0^\infty r^2dr\,[g_a(r)g_b(r) + f_a(r)f_b(r)]\left\{e^2\int_0^\infty r'^2dr'\frac{\rho_p(r')}{r_>}\right\}\frac{(1+q_a)}{2}\frac{(1+q_b)}{2}, \tag{27}$$

with the definitions

$$\rho(r) = \frac{1}{4\pi}\sum_a \hat{j}_a^2\,[g_a^2(r) + f_a(r)^2] \,,$$
$$\rho_s(r) = \frac{1}{4\pi}\sum_a \hat{j}_a^2\,[g_a^2(r) - f_a(r)^2] \,, \tag{28}$$

for the baryon and scalar density in finite nuclei, where $\hat{j} = \sqrt{2j+1}$ and index a running over all occupied orbits. If the baryon density of the protons $\rho_p(r)$ is needed as in the Coulomb self-energy Σ_c^H, index a runs only over occupied proton orbits. Note the use of the coupling constants depending on the local position, which is just an abbreviation for $G_i(r) = G_i(\rho(r))$. In Eqs. (25)–(27) $r_<$ and $r_>$ denote the smaller or bigger value of r and r'. The functions $\widetilde{I}_L(x)$ and $\widetilde{K}_L(x)$ arise from the multipole expansion of the meson propagator in coordinate space and are defined using the modified spherical Bessel functions I and K [22]:

$$\widetilde{I}_L(x) = \frac{I_{L+1/2}(x)}{\sqrt{x}}, \quad \widetilde{K}_L(x) = \frac{K_{L+1/2}(x)}{\sqrt{x}} . \tag{29}$$

The Fock contributions originating from the σ exchange read

$$\langle\alpha|\Sigma_\sigma^F|\beta\rangle = \delta_{\kappa_a,\kappa_b}\delta_{m_a,m_b}\delta_{q_a,q_b}\frac{(-m_\sigma)}{\hat{j}_a^2}\sum_c \delta_{q_a,q_c}\int_0^\infty r^2dr\Big\{G_\sigma(r)\,[g_a(r)g_c(r) - f_a(r)f_c(r)]$$
$$\times\int_0^\infty r'^2dr'G_\sigma(r')\,[g_c(r')g_b(r') - f_c(r')f_b(r')]\sum_L\langle a||Y_L||c\rangle^2\widetilde{I}_L(m_\sigma r_<)\widetilde{K}_L(m_\sigma r_>)\Big\}\,, \tag{30}$$

with index c running over all occupied states. Here and in the following expressions for the other mesons the $\langle a||Y_L||b\rangle$ represent the reduced matrix elements of the spherical harmonics and

$$\langle a||T_J(L)||b\rangle = \sqrt{\frac{6}{4\pi}}(-)^{l_a}\hat{l}_a\hat{l}_b\hat{j}_a\hat{j}_b\hat{L}\hat{J}\begin{pmatrix} l_a & L & l_b \\ 0 & 0 & 0\end{pmatrix}\begin{Bmatrix} j_a & j_b & J \\ l_a & l_b & L \\ \frac{1}{2} & \frac{1}{2} & 1\end{Bmatrix}. \tag{31}$$

Using this notation, the matrix elements of the Fock contributions arising from the ω exchange can be written

$$\langle\alpha|\Sigma_\omega^F|\beta\rangle = \delta_{\kappa_a,\kappa_b}\delta_{m_a,m_b}\delta_{q_a,q_b}\frac{m_\omega}{\hat{j}_a^2}\sum_c\delta_{q_a,q_c}$$
$$\times\Big\{\int_0^\infty r^2drG_\omega(r)\,[g_a(r)g_c(r) + f_a(r)f_c(r)]\int_0^\infty r'^2dr'G_\omega(r')\,[g_c(r')g_b(r') + f_c(r')f_b(r')]$$
$$\times\sum_L\langle a||Y_L||c\rangle^2\widetilde{I}_L(m_\omega r_<)\widetilde{K}_L(m_\omega r_>)\Big\} + \sum_{LJ}\Big\{\int_0^\infty r^2drG_\omega(r)\big[g_a(r)f_c(r)\langle c'||T_J(L)||a\rangle$$
$$-f_a(r)g_c(r)\langle c||T_J(L)||a'\rangle\big]\int_0^\infty r'^2dr'G_\omega(r')\big[g_c(r')f_b(r')\langle c||T_J(L)||a'\rangle$$
$$-f_c(r')g_b(r')\langle c'||T_J(L)||a\rangle\big]\widetilde{I}_L(m_\omega r_<)\widetilde{K}_L(m_\omega r_>)\Big\}\,. \tag{32}$$

The isovector pseudoscalar meson using the pseudovector coupling yields

$$\langle\alpha|\Sigma_\pi^F|\beta\rangle = \delta_{\kappa_a,\kappa_b}\delta_{m_a,m_b}\delta_{q_a,q_b}\left(\frac{f_\pi}{m_\pi}\right)^2\frac{1}{\hat{j}_a^2}\sum_c(2-\delta_{q_a,q_c})$$
$$\times\int_0^\infty r^2dr\Big\{-\frac{\hat{j}_a^2\hat{j}_b^2}{8\pi}\,[g_a(r)g_c(r) + f_a(r)f_c(r)]\,[g_b(r)g_c(r) + f_b(r)f_c(r)]$$
$$+m_\pi^3\sum_L\hat{L}^{-4}|\langle a||Y_L||c'\rangle|^2\sum_{L_1L_2}i^{L_2-L_1}\,[\{\kappa_a+\kappa_c+h(L_1)\}g_a(r)g_c(r) - \{\kappa_a+\kappa_c-h(L_1)\}f_a(r)f_c(r)]$$
$$\times\int_0^\infty r'^2dr'[\{\kappa_b+\kappa_c+h(L_2)\}g_b(r)g_c(r) - \{\kappa_b+\kappa_c-h(L_2)\}f_b(r)f_c(r)]R(L_1,L_2,r,r')$$
$$+\frac{1}{3}\sum_{LJ}[\langle a||T_J(L)||c\rangle g_a(r)g_c(r) + \langle a'||T_J(L)||c'\rangle f_a(r)f_c(r)]$$
$$\times\,[\langle a||T_J(L)||c\rangle g_b(r)g_c(r) + \langle a'||T_J(L)||c'\rangle f_b(r)f_c(r)]\Big\}\,, \tag{33}$$

with $L_i = \{L-1, L+1\}$ and the auxiliary functions

$$h(L_i) = \begin{cases} -L & \text{if } L_i = L-1\,, \\ L+1 & \text{if } L_i = L+1\,, \end{cases} \tag{34}$$

$$R(L_1,L_2,r,r') = \theta(r'-r)\widetilde{I}_{L_1}(m_{ps}r)\widetilde{K}_{L_2}(m_{ps}r') + \theta(r-r')\widetilde{I}_{L_2}(m_{ps}r')\widetilde{K}_{L_1}(m_{ps}r)\,, \tag{35}$$

using the step function $\theta(x-y)$. The expressions for the self-energy show that the Hartree contributions can be rewritten by defining a local potential, e.g.,

$$\langle\alpha|\Sigma^H_\sigma|\beta\rangle = \delta_{\kappa_a,\kappa_b}\delta_{m_a,m_b}\delta_{q_a,q_b}\int_0^\infty r^2dr\,[g_a(r)g_b(r)-f_a(r)f_b(r)]\,V_\sigma(r)$$
$$= \delta_{\kappa_a,\kappa_b}\delta_{m_a,m_b}\delta_{q_a,q_b}\int d^3r\Psi^\dagger_\alpha(r)\gamma^0V_\sigma(r)\Psi_\beta(r), \tag{36}$$

with

$$V_\sigma(r) = -G_\sigma(r)m_\sigma\int_0^\infty r'^2dr'\rho_s(r')G_\sigma(r')\tilde{I}_0(m_\sigma r_<)\tilde{K}_0(m_\sigma r_>)\ , \tag{37}$$

whereas the Fock contributions are obviously nonlocal.

Solving the Dirac equation (5) with the technique mentioned above in a self-consistent way one can finally determine the binding energy of the nucleus with A nucleons as

$$E = \frac{1}{2}\sum_{\alpha,(\mathrm{occ})}E_\alpha + T_\alpha \quad - AM\ , \tag{38}$$

where E_α denotes the single-particle energy obtained by solving the Dirac equation and T_α is the corresponding kinetic energy.

III. LOCAL-DENSITY APPROXIMATION

In contrast to the effective meson-exchange approach, which, as discussed in the preceding section, determines the effects of correlations from studies of nuclear matter, we are now considering an approximation in which the relativistic effects are deduced from nuclear matter. For that purpose we consider as an example the expansion of an harmonic oscillator (HO) state in terms of plane wave spinors,

$$\Psi_{n,j,l,m}(\mathbf{p},\rho) = \sqrt{\frac{E^*(\mathbf{p},\rho)+M^*(\mathbf{p},\rho)}{2E^*(\mathbf{p},\rho)}}\begin{pmatrix} 1 & \mathcal{Y}_{jlm}(\Omega_p) \\ \frac{\boldsymbol{\sigma}\cdot\mathbf{p}^*(\rho)}{[E^*(p,\rho)+M^*(p,\rho)]} & \mathcal{Y}_{jl'm}(\Omega_p)\end{pmatrix}\Phi_{n,l}(p), \tag{39}$$

where $\Phi_{n,l}(p)$ are the momentum space HO wave functions. The structure of the plane wave Dirac spinor, in particular the ratio of the small to large component, is determined by the quantities p^*, M^* and E^* as defined in Eq. (8). The values actually used for these quantities are taken from the DBHF calculations at a density ρ for the realistic NN interaction under consideration. In this sense the Dirac structure of the harmonic oscillator state defined in Eq. (39) is derived from nuclear matter of a given density ρ. For the Dirac spinors as presented in Eq. (39) one can calculate the matrix elements of the OBE potential under consideration employing the conventional techniques and identify the resulting numbers with matrix elements of a two-body interaction V between nonrelativistic harmonic oscillator states,

$$\langle\alpha\beta|V(\rho)|\gamma\delta\rangle\ , \tag{40}$$

where $\alpha\cdots\delta$ refer to the quantum numbers of the various HO states and the parameter ρ is kept to memorize that the value of this matrix element depends on a density parameter ρ, which determines the Dirac structure of the spinors used to calculate the matrix element. This scheme can of course be generalized to single-particle wave functions different from HO functions. In a corresponding way one can also evaluate the matrix elements for the operator of the kinetic energy,

$$t_{\alpha\beta}(\rho) = \int d^3p\Psi^\dagger_\alpha\left[\boldsymbol{\gamma}\cdot\mathbf{p}+M\right]\Psi_\beta - M\delta_{\alpha\beta}$$
$$= \int d^3p\Phi^*_\alpha\left[\frac{MM^*(\rho)+pp^*(\rho)}{E^*(\rho)}-M\right]\Phi_\beta\ . \tag{41}$$

For the interaction defined by the matrix elements of Eq. (40) one may now solve the Bethe-Goldstone equation

$$G(Z,\rho) = V(\rho) + V(\rho)\frac{Q}{Z-QH_0Q}G(Z,\rho)\ , \tag{42}$$

using the standard techniques of nonrelativistic BHF calculations for finite nuclei [23]. The Pauli operator Q in this equation is defined in terms of HO states appropriate for the nucleus under consideration. Beside the usual dependence on the starting energy Z, the matrix elements of G also depend on the density parameter ρ characterizing the structure of the Dirac spinors involved. Keeping track of this additional density dependence one can expand the BHF single-particle states $|i\rangle$ and $|j\rangle$ in the basis of HO states $|\alpha\rangle$,

$$|i\rangle = \sum_\alpha c_{i\alpha}|\alpha\rangle\ , \tag{43}$$

and the expansion coefficients are determined from the solution of the eigenvalue problem

$$\sum_{\beta}\left[t_{\alpha\beta}(\rho_i)+\sum_{j,(\mathrm{occ})}\langle\alpha j|G(Z=\epsilon_i+\epsilon_j,\rho_{ij})|\beta j\rangle\right]c_{i\beta}=\epsilon_i c_{i\alpha}\ . \tag{44}$$

If one ignores in this equation the medium dependence of the Dirac spinors by putting ρ_i and ρ_{ij} equal to zero, this Eq. (44) together with the Bethe-Goldstone equation (42) defines the conventional BHF approach for realistic OBE potentials [24]. In addition to the self-consistency requirements of this BHF approach, we now want to account for the medium dependence of the Dirac spinors and define an average density for nucleons in the orbit i by

$$\rho_i=\int d^3r\ \phi_i^*(r)\rho_{\mathrm{DBHF}}(r)\phi_i(r)\ , \tag{45}$$

with $\phi_i(r)$ the DBHF single-particle wave function and $\rho_{\mathrm{DBHF}}(r)$ the radial shape of the baryon density obtained from this calculation. This average single-particle density enters into the calculation of the kinetic energy and it is also used to define the average density for an interacting pair of nucleons by

$$\rho_{ij}=\sqrt{\rho_i\rho_j}\ . \tag{46}$$

IV. RESULTS AND DISCUSSION

As a first step towards the application of the effective meson-exchange approach discussed in Sec. II, we have to determine the coupling constants $G_\sigma(\rho)$ and $G_\omega(\rho)$, depending on the baryon density ρ. As discussed in Sec. II A this is done by adjusting these parameters in such a way that a mean-field calculation reproduces at each density the results for the scalar self-energy Σ^s and the binding energy per nucleon obtained in DBHF calculations for nuclear matter [25]. For the mean-field calculation we consider three different approximations. In the first approach, we just consider the Hartree contributions to the self-energy and total energy [see Eqs. (13) and (13)]. In the second approach we consider a σ-ω model in the Hartree-Fock approximation; i.e., we keep the Hartree-Fock terms in Eqs. (13) and (14) which originate from the exchange of a σ or ω meson. This approach will be called HF(σ,ω) or HF1. In the approach HF2 or HF(σ,ω,π) we furthermore consider the effects of the pion exchange, which means that we are considering the complete set outlined in Sec. II.

Results for the effective coupling constants determined from DBHF calculations for OBE potentials A and C [2,25], are listed in Table I for various densities. For all three approaches considered, the effective coupling constants G_σ and G_ω decrease with increasing density. This is also displayed in Fig. 1. The decrease reflects the fact that the terms in the G-matrix, which are of second and higher order in the interaction, contain contributions which are simulated by the exchange of a scalar and a vector meson [26]. Due to the Pauli operator in the Bethe-Goldstone equation (42) and due to the change in the energy dominator, these contributions of higher order in the bare interaction V are quenched with increasing density. The importance of the density-dependent correlation effects parametrized in terms of these coupling constants is reflected by the fact that the square of the coupling constants is quenched by a factor 2, if the nuclear density is increased from $0.2\rho_0$ to $1.4\rho_0$ (ρ_0 denoting the empirical saturation density).

Such a substantial density dependence of the effective coupling constants of course affects the nuclear structure calculations. This is displayed in Fig. 2, where the results for the binding energy per nucleon and the effective mass of the nucleon determined in a DBHF calculation

TABLE I. DBHF results for nuclear matter derived from the OBE potential A for the scalar part of nucleon self-energy (Σ^s) and the binding energy per nucleon (E/A) for various Fermi momenta k_f. The columns G_σ and G_ω show the coupling constants which are needed to reproduce these results in a HF calculation. For this purpose three different models are considered: the Hartree approximation ignoring the all Fock contributions to the self-energy and binding energy (model "Hart"), the Hartree-Fock approximation ignoring the contribution of the pion exchange (model "HF1"), and the full model defined in Sec. II A (model "HF2"). All energies are listed in MeV and the Fermi momenta in units fm^{-1}. For a comparison the lowest part of the table also shows results obtained for the OBE potential C at one specific density.

k_F	E/A	Σ^s	Model	G_σ	G_ω
0.80	-7.27	-134.3	Hart	12.436	15.403
			HF1	11.411	12.941
			HF2	11.227	13.179
1.00	-10.62	-209.8	Hart	11.177	13.807
			HF1	10.265	11.668
			HF2	10.104	11.885
1.20	-13.44	-288.8	Hart	10.059	12.322
			HF1	9.267	10.470
			HF2	9.118	10.674
1.40	-15.59	-374.9	Hart	9.224	11.168
			HF1	8.531	9.539
			HF2	8.389	9.733
1.50	-14.88	-416.3	Hart	8.851	10.673
			HF1	8.197	9.145
			HF2	8.048	9.336
			OBE potential C		
1.20	-11.57	-292.8	Hart	10.130	12.534
			HF1	9.297	10.669
			HF2	9.149	10.869

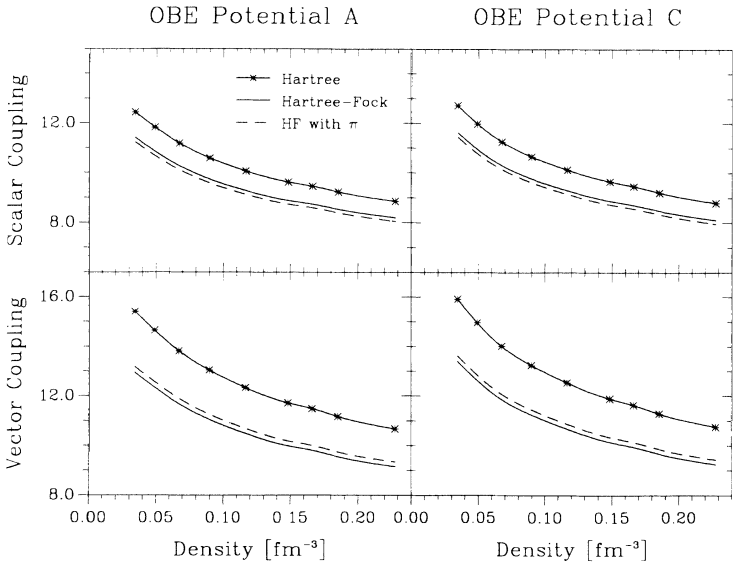

FIG. 1. Effective coupling constants for the exchange of a scalar meson (G_σ) and vector meson (G_ω) as a function of the density. The coupling constants are derived from DBHF calculations of nuclear matter employing the OBE potentials A (left part) and C (right part). Various mean-field approximations are considered: the Hartree approximation, the Hartree-Fock approximation with only σ and ω exchange (HF1), and the complete model of Sec. II, also including the pion (HF2).

are compared to the corresponding quantities obtained in Hartree calculations using effective coupling constants which are determined to reproduce the DBHF results at a small density (dashed curve) or large density (dotted line). It is obvious that the large coupling constant G_σ determined for small densities predicts an effective mass at larger density which is considerably smaller than the one obtained in the self-consistent DBHF calculation. This is an example to demonstrate that mean-field calculations employing constant coupling constants tend to overestimate the change of the Dirac spinors in nuclear matter at high densities.

The density-dependent coupling constants also affect the predictions for the saturation properties of nuclear matter. Note that the energy versus density curve obtained from the Hartree calculation with coupling constant appropriate for small densities yields a minimum at a low density and overestimates the binding energy by about 8 MeV per nucleon. The Hartree calculations using coupling constants for large densities (dotted line in Fig. 2) predict a minimum at higher densities and a lower energy per nucleon. Therefore the minima of the energy versus density curves obtained from coupling constants determined at various densities form a "band" of saturation points, which is perpendicular to the "Coester band."

The same phenomenon can also be observed in calculations of finite nuclei. This is demonstrated in Table II where we show results of relativistic Hartree-Fock calculations considering coupling constants as derived from various densities in nuclear matter. The binding energies displayed in this table and all subsequent ones are corrected for spurious center of mass effects, assuming a harmonic oscillator model, and the radius of the charge distribution has been evaluated from the proton density, assuming a radius of 0.8 fm for the charge radius of the proton.

Inspecting the results displayed in Table II one observes a sensitive dependence of the calculated binding energy on the choice for the coupling constants. This demonstrates again the importance of the density-dependent correlation effects contained in the G matrix of nuclear matter. It is striking to see that the calculation which yields the largest binding energy ($\rho = 0.2\rho_0$) also predicts the largest radius of the charge distribution. So we find also for finite nuclei that the ground-state properties of finite nuclei calculated with meson-exchange parameters derived from various densities form

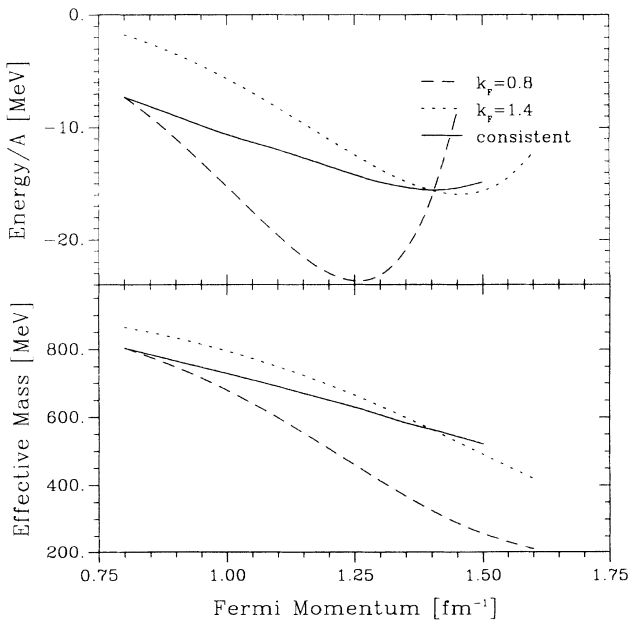

FIG. 2. Results for the binding energy per nucleon (upper part) and the effective mass M^* of the nucleon as a function of the Fermi momentum in nuclear matter. Results obtained from DBHF calculations (OBE potential A, solid line) are compared to those of Hartree calculations in which the effective coupling constants are determined to reproduce the DBHF results at $\rho = 0.2\rho_0$ (k_F=0.8, long dashed line) and at $\rho = 1.1\rho_0$ (k_F=1.40, dotted line).

TABLE II. Results of relativistic HF calculations on ^{16}O, considering the exchange of effective σ, ω, and π mesons. The coupling constants are determined to reproduce DBHF results for nuclear matter (OBE potential A) at various densities: $\rho = 0.2\rho_0$ (k_F=0.8 fm^{-1}), $\rho = 0.5\rho_0$ (k_F=1.1 fm^{-1}), and $\rho = 1.4\rho_0$ (k_F=1.5 fm^{-1}). These results can be compared to those of a self-consistent calculation (last column) considering local coupling constants as discussed in Sec. II B. Results are presented for the single-particle energies of proton states, the binding energy per nucleon (E/A, corrected for c.m. effects), and the radius of the charge distribution ($R_{\rm ch}$).

	$\rho = 0.2\rho_0$	$\rho = 0.5\rho_0$	$\rho = 1.4\rho_0$	Self-consistent
$\epsilon_{s1/2}$ [MeV]	-54.4	-48.8	-46.6	-47.1
$\epsilon_{p3/2}$ [MeV]	-33.9	-25.4	-20.1	-23.8
$\epsilon_{p1/2}$ [MeV]	-18.6	-13.7	-11.3	-17.7
E/A [MeV]	-15.17	-9.29	-5.38	-7.73
$R_{\rm ch}$ [fm]	2.52	2.46	2.37	2.48

a "band" which is perpendicular to the normal "Coester band" [24].

Furthermore, it is worth noting that the spin-orbit splitting deduced from the difference in the single-particle energies $\epsilon_{p3/2}$ and $\epsilon_{p1/2}$ is of course largest for that interaction which yields the smallest effective mass in nuclear matter ($\rho = 0.2\rho_0$). The comparison displayed in Table II demonstrates the importance of relativistic effects for the spin-orbit splitting in the nuclear shell model [27].

Table II also contains a first result which is obtained when we consider an effective meson exchange with local coupling constants, depending on the position of the interacting nucleons as discussed in Sec. II B. As to be expected, one finds that the single-particle energy for the $p_{1/2}$ state obtained in this self-consistent calculation is closer to the one obtained $\rho = 0.2\rho_0$, while the single-particle energy of the deep lying $s_{1/2}$ state is closer to the one obtained at larger densities. It should be mentioned that effective coupling constants can safely be derived from nuclear matter calculations only for densities as low as $\approx$ 0.2 times the saturation density ρ_0. For smaller densities the conventional tools to evaluate BHF energies yield unstable results [11]. Therefore we extrapolate the coupling constants to smaller densities using spline functions in terms of the density.

The next question we want to investigate is the sensitivity of the effective meson-exchange model on the mesons taken into account. For that purpose we have performed Hartree calculations for finite nuclei using the local coupling constants as derived from the Hartree calculations of nuclear matter (column "Hart" in Table I). In the same way we also perform HF calculations for finite nuclei, taking into account the effects of σ and ω exchange using the density-dependent coupling constants derived from nuclear matter ("HF1") and finally consider the complete model with inclusion of the pion discussed in Sec. II ("HF2").

Results obtained for these three effective meson-exchange models for the nuclei ^{16}O, ^{40}Ca, and ^{48}Ca are displayed in Tables III, IV, and V, respectively. Using the OBE potential A, which yields a correct description of the saturation point of nuclear matter, the Hartree approximation shows fair agreement with the experimental data for the binding energy and radius of all three nuclei considered. Both the results for the radius and the binding energy are slightly below the experimental values. Employing potential C yields larger radii but smaller binding energies. This is the typical feature for two phase-shift equivalent potentials; the results change along the "Coester band."

TABLE III. Results of relativistic HF calculations on ^{16}O, considering various models for the effective meson exchange (Hart, HF1, HF2; see Table I) are compared to results of conventional BHF calculations and BHF calculations which account for Dirac effects in the way described in Sec. III (DBHF). Further information see Table II .

	Hart.	HF1	HF2	BHF	DBHF	Expt.
			Potential A			
$\epsilon_{s1/2}$ [MeV]	-44.0	-44.0	-47.1	-56.6	-49.8	-40±8
$\epsilon_{p3/2}$ [MeV]	-21.5	-23.4	-23.8	-25.7	-23.0	-18.4
$\epsilon_{p1/2}$ [MeV]	-15.8	-15.8	-17.7	-17.4	-13.1	-12.1
E/A [MeV]	-7.20	-7.23	-7.73	-5.95	-7.56	-7.98
$R_{\rm ch}$ [fm]	2.57	2.48	2.48	2.31	2.46	2.70
			Potential C			
$\epsilon_{s1/2}$ [MeV]	-37.0	-37.4	-40.2	-45.2	-40.9	-40±8
$\epsilon_{p3/2}$ [MeV]	-17.7	-19.4	-19.7	-19.5	-18.0	-18.4
$\epsilon_{p1/2}$ [MeV]	-13.3	-13.5	-14.9	-13.7	-11.0	-12.1
E/A [MeV]	-5.60	-5.59	-6.09	-4.03	-5.30	-7.98
$R_{\rm ch}$ [fm]	2.73	2.62	2.62	2.48	2.59	2.70

TABLE IV. Results of relativistic HF calculations on ^{40}Ca. Further information see Table III.

	Hart.	HF1	HF2	BHF	DBHF	Expt.
			Potential A			
$\epsilon_{d5/2}$ [MeV]	-19.8	-21.0	-20.8	-30.2	-21.9	-14±2
$\epsilon_{1s1/2}$ [MeV]	-15.4	-13.7	-14.1	-24.5	-13.8	-10±1
$\epsilon_{d3/2}$ [MeV]	-14.5	-13.2	-14.2	-16.5	-10.2	-7±1
E/A [MeV]	-8.21	-7.76	-8.09	-8.29	-8.64	-8.50
$R_{\rm ch}$ [fm]	3.35	3.14	3.14	2.64	3.05	3.50
			Potential C			
$\epsilon_{d5/2}$ [MeV]	-15.3	-16.9	-16.7	-21.0	-16.5	-14±2
$\epsilon_{1s1/2}$ [MeV]	-10.9	-11.3	-11.5	-16.9	-10.6	-10±1
$\epsilon_{d3/2}$ [MeV]	-10.5	-10.8	-11.5	-12.0	-8.0	-7±1
E/A [MeV]	-5.83	-5.80	-6.14	-5.06	-5.91	-8.55
$R_{\rm ch}$ [fm]	3.44	3.31	3.32	2.87	3.21	3.50

The inclusion of the Fock terms in HF1 reduces the calculated radii to a significant extent, predicting the same or a slightly smaller binding energy as compared to the Hartree approach. Therefore the agreement with experiment gets worse. Furthermore, we note that the Fock terms tend to enhance the spin-orbit splitting in the single-particle energies, which again deteriorates the agreement with the splitting observed in the experimental data.

The pion-exchange terms included in the HF2 approximation slightly improve the agreement between calculation and experiment. The spin-orbit splitting is reduced and the binding energies are larger but the results for the radii are essentially the same as in the HF1 approximation. Keeping in mind the sensitivity of the calculated values on the density dependence of the effective coupling constants displayed in Table II and discussed above, one may conclude, however, that all three models lead to results which are rather similar.

The main purpose of this study is to compare the predictions of the effective meson-exchange approach to the results obtained in BHF calculations, which treat the change of the Dirac spinors in the medium in a local-density approximation (see Sec. III and Ref. [20]). For that purpose Tables III and IV show results of this approach (identified as DBHF) and allow a comparison with conventional BHF calculations, which ignore medium dependence of the Dirac spinors completely. The differences between BHF and DBHF results are by far not as large as those displayed in Table II, which reflect the density dependence of the correlations. Therefore we conclude that the bulk properties of nuclei are more sensitive to the density dependence of the correlations than to the medium dependence of the Dirac spinors. That is why we consider the approach which treats the Dirac effects in a local-density approximation (DBHF), to give more reliable predictions for a complete Dirac-Brueckner-Hartree-Fock calculation than the effective meson-exchange approach, which derives the correlation effects from nuclear matter.

For the case of the nucleus ^{16}O it has already been shown in [20] that the inclusion of Dirac effects in DBHF leads to larger radii and binding energies as compared to the predictions of conventional BHF calculations. Thereby the agreement of the theoretical predictions is substantially improved. This observation is supported by the results on ^{40}Ca shown in Table IV. Furthermore, one finds that the DBHF results are in fair agreement with those obtained in the relativistic HF approximation using effective meson exchange. This agreement supports the conclusion that both types of approaches are reliable approximations for a complete Dirac-Brueckner calculation.

Finally, we want to investigate the basic assumption of the DBHF approach which assumes that the Dirac spinors for the single-particle states in finite nuclei can be described in terms of plane wave spinors of nuclear matter. For that purpose we consider as an example the radial functions $g_a(r)$ and $f_a(r)$ for the large and small component of the $0s_{1/2}$ Dirac spinor calculated in a relativistic HF approach (HF1, OBEPA) for ^{40}Ca (see solid lines in Fig. 3). For the comparison we consider a Dirac spinor expanded in terms of spinors for nuclear matter assuming a harmonic oscillator expansion as in Eq. (39). If we consider plane wave Dirac spinors of the vacuum (k_F=0, dotted line), the lower or small component is considerably weaker than the one resulting from the relativistic HF calculation. For the appropriate average density ρ_i as defined in Eq. (45) the enhancement of the small component in the medium is fairly well described. This demonstrates that the two approaches not only lead to very similar results for the global observables like binding energy and radius, but also provide similar predictions for the components of the Dirac spinors.

TABLE V. Results of relativistic HF calculations on ^{48}Ca using the OBE potential A. Further information see Table III.

	Hart.	HF1	HF2	Expt.
$\epsilon_{d5/2}$ [MeV]	-24.6	-29.0	-27.2	-20±1
$\epsilon_{1s1/2}$ [MeV]	-18.7	-19.5	-20.2	-15.8
$\epsilon_{d3/2}$ [MeV]	-19.5	-21.6	-25.1	-15.3
E/A [MeV]	-8.35	-7.83	-7.90	-8.70
$R_{\rm ch}$ [fm]	3.34	3.15	3.16	3.50

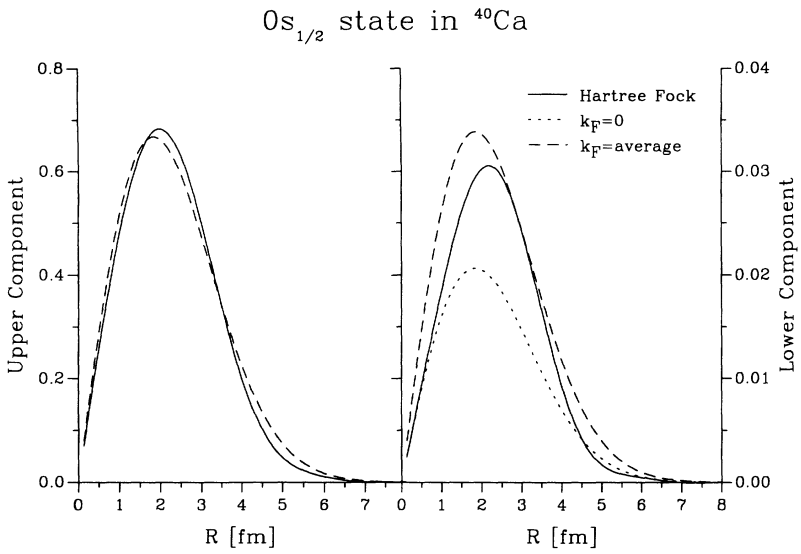

FIG. 3. The radial functions for the large upper component $g(r)$ and the small lower component $f(r)$ (both multiplied by r) for the $0s_{1/2}$ Dirac spinor obtained in a relativistic HF calculation (HF1, OBEPA) for ^{40}Ca are compared to a harmonic oscillator spinor of Eq. (39) assuming no medium correction ($k_F = 0$, dotted line) or as predicted by nuclear matter at an average density (dashed line).

V. CONCLUSIONS

Two different steps towards a self-consistent Dirac-Brueckner calculation for finite nuclei are presented and discussed. In the effective meson-exchange approximation one solves the relativistic Hartree-Fock equations directly for the finite system and deduces the correlation effects from nuclear matter. This is done in various models to study the importance of Fock exchange effects and the impact of the pion exchange. The density dependence of the effective coupling constants reflects the density dependence of the correlations encountered in the Brueckner G matrix.

In an alternative approach (DBHF) the correlation effects are treated directly for the finite nuclei but the change of the Dirac spinors is determined from nuclear matter. It is demonstrated that the bulk properties of nuclei (binding energy and radius) are less affected by the change of the Dirac spinors than by the density dependence of the correlations. This implies that the approach which treats the correlation effects without an approximation should provide more reliable results than the effective meson-exchange approach.

It turns out that both approximations yield very similar results. For the realistic OBE potential A defined in [2] binding energies per nucleon are obtained for ^{16}O, ^{40}Ca, and ^{48}Ca, which are close to the experimental value ($\pm$ 0.5 MeV). The predictions for the radii are still significantly below the experimental data (typically 0.2 fm). This might be improved by including correlations beyond the lowest order Brueckner theory. Recently it has been demonstrated that the inclusion of hole-hole scattering terms within a self-consistent Green function approach tends to improve BHF results in this direction [28].

ACKNOWLEDGMENTS

This work has partly been supported by the Graduiertenkolleg "Struktur und Wechselwirkung von Hadronen und Kernen," Tübingen (DFG, Mu705/3-1).

[1] R. Machleidt, K. Holinde, and C. Elster, Phys. Rep. **149**, 1 (1987).
[2] R. Machleidt, Adv. Nucl. Phys. **19**, 189 (1989).
[3] B.D. Serot and J. D. Walecka, Adv. Nucl. Phys. **16**, 1 (1986).
[4] K.T.R. Davies, M. Baranger, R.M. Tarbutton, and T.T.S. Kuo, Phys. Rev. **177**, 1519 (1969).
[5] R.K. Tripathi, A. Faessler, and H. Müther, Phys. Rev. C **10**, 2080 (1974).
[6] F. Coester, S. Cohen, B.D. Day, and C.M. Vincent, Phys. Rev. C **1**, 769 (1970).
[7] H. Müther, Prog. Part. Nucl. Phys. **14**, 123 (1985).
[8] B.D. Day and R.B. Wiringa, Phys. Rev. C **32**, 1057 (1985).
[9] V.R. Pandharipande and R.B. Wiringa, Rev. Mod. Phys. **51**, 821 (1979).
[10] H. Kümmel, K.H. Lührmann, and J.G. Zabolitzky, Phys. Rep. **36**, 1 (1978).
[11] W.H. Dickhoff and H. Müther, Rep. Prog. Phys. **11**, 1946 (1992).
[12] H.Q. Song, S.D. Yang, and T.T.S. Kuo, Nucl. Phys. **A462**, 491 (1987).
[13] M.R. Anastasio, L.S. Celenza, W.S. Pong, and C.M. Shakin, Phys. Rep. **100**, 327 (1978); L.S. Celenza and C.M. Shakin, *Relativistic Nuclear Physics* (World Scientific, Singapore, 1986).
[14] R. Brockmann and R. Machleidt, Phys. Lett. **149B**, 283 (1984).
[15] B. ter Haar and R. Malfliet, Phys. Rep. **149**, 207 (1987).
[16] C. J. Horowitz and B. D. Serot, Phys. Lett. **137B**, 287 (1984); Nucl. Phys. **A464**, 613 (1987).
[17] A. Bouyssy, J.-F. Mathiot, Nguyen van Giai, and S. Marcos, Phys. Rev. C **36**, 380 (1987).
[18] R. Brockmann and H. Toki, Phys. Rev. Lett. **68**, 3408

(1992).
[19] R. Fritz, H. Müther, and R. Machleidt, Phys. Rev. Lett. **71**, 46 (1993).
[20] H. Müther, R. Machleidt, and R. Brockmann, Phys. Lett. B **202**, 483 (1988); Phys. Rev. C **42**, 1981 (1990).
[21] R. Fritz (unpublished).
[22] *Handbook of Mathematical Functions*, edited by M. Abramowitz and I.A. Stegun (Dover, New York, 1970).
[23] H. Müther and P.U. Sauer, *Computational Nuclear Physics 2* (Springer, New York, 1993), p. 30.
[24] K.W. Schmid, H. Müther, and R. Machleidt, Nucl. Phys. **A530**, 14 (1991).
[25] R. Brockmann and R. Machleidt, Phys. Rev. C **42**, 1965 (1990).
[26] H. Elsenhans, H. Müther, and R. Machleidt, Nucl. Phys. **A515**, 715 (1990).
[27] L. Zamick, D.C. Zheng, and H. Müther, Phys. Rev. C **45**, 2763 (1992).
[28] H. Müther and L. Skouras (unpublished).